

Single CA3 pyramidal cells trigger sharp waves *in vitro* by exciting interneurons

Michaël Bazélot, Maria T. Teleńczuk and Richard Miles

Inserm U1127, CNRS UMR7225, Sorbonne Universités, UPMC Univ Paris 6 UMR S1127, Institut du Cerveau et de la Moelle épinière, Paris, France

Key points

- The CA3 hippocampal region generates sharp waves (SPW), a population activity associated with neuronal representations. The synaptic mechanisms responsible for the generation of these events still require clarification.
- Using slices maintained in an interface chamber, we found that the firing of single CA3 pyramidal cells triggers SPW like events at short latencies, similar to those for the induction of firing in interneurons.
- Multi-electrode records from the CA3 stratum pyramidale showed that pyramidal cells triggered events consisting of putative interneuron spikes followed by field IPSPs. SPW fields consisted of a repetition of these events at intervals of 4–8 ms. Although many properties of induced and spontaneous SPWs were similar, the triggered events tended to be initiated close to the stimulated cell.
- These data show that the initiation of SPWs *in vitro* is mediated via pyramidal cell synapses that excite interneurons. They do not indicate why interneuron firing is repeated during a SPW.

Abstract Sharp waves (SPWs) are a hippocampal population activity that has been linked to neuronal representations. We show that SPWs in the CA3 region of rat hippocampal slices can be triggered by the firing of single pyramidal cells. Single action potentials in almost one-third of pyramidal cells initiated SPWs at latencies of 2–5 ms with probabilities of 0.07–0.76. Initiating pyramidal cells evoked field IPSPs (fIPSPs) at similar latencies when SPWs were not initiated. Similar spatial profiles for fIPSPs and middle components of SPWs suggested that SPW fields reflect repeated fIPSPs. Multiple extracellular records showed that the initiated SPWs tended to start near the stimulated pyramidal cell, whereas spontaneous SPWs could emerge at multiple sites. Single pyramidal cells could initiate two to six field IPSPs with distinct amplitude distributions, typically preceded by a short-duration extracellular action potential. Comparison of these initiated fields with spontaneously occurring inhibitory field motifs allowed us to identify firing in different interneurons during the spread of SPWs. Propagation away from an initiating pyramidal cell was typically associated with the recruitment of interneurons and field IPSPs that were not activated by the stimulated pyramidal cell. SPW fields initiated by single cells were less variable than spontaneous events, suggesting that more stereotyped neuronal ensembles were activated, although neither the spatial profiles of fields, nor the identities of interneurons firing were identical for initiated events. The effects of single pyramidal cell on network events are thus mediated by different sequences of interneuron firing.

(Resubmitted 1 October 2015; accepted after revision 22 December 2015; first published online 5 January 2016)

Corresponding authors R. Miles, Inserm U1127, ICM, CHU Pitié-Salpêtrière, 47 Boulevard de l'Hôpital, Paris 75013, France. Email: richard.miles@upmc.fr

M. Bazélot, GW Pharmaceuticals, Porton Down Science Park, Porton Down, Salisbury SP4 0JQ, UK. Email: mbazelot@gwpharm.com

Abbreviations DAMGO, (D-Ala² N-MePhe⁴ Gly-ol)-enkephalin; fIPSP, field inhibitory post-synaptic potential; SPW, sharp wave.

Introduction

Single mammalian pyramidal cells are not considered to have major effects on the cortical networks to which they belong (Shadlen & Newsome, 1998). Even so, single pyramidal cells of layers 5 and 6 of the motor cortex can induce or affect whisker movements (Brecht *et al.* 2004), whereas stimulation of single layer 5 somatosensory pyramidal cells modifies behavioural responses during a detection task (Houweling & Brecht, 2008). Single neurones can also modify the collective activities of cortical neuronal populations. In the somatosensory or visual cortex, single cells can induce transitions between cortical up and down states (Li, Poo & Dan, 2009). The firing of a single GABAergic inhibitory cell can alter the timing of population events in the immature hippocampus (Bonifazi *et al.* 2009), whereas some pyramidal cells entrain or initiate epileptiform population events in the adult hippocampus (Miles & Wong, 1983; Prida *et al.* 2006).

Sharp waves (SPWs) are hippocampal EEG events with a duration of 30–60 ms (O'Keefe & Nadel, 1978; Buzsaki, Leung & Vanderwolf, 1983) that occur during behaviours including awake immobility and slow wave sleep. Buzsaki *et al.* (1992) showed that SPWs are accompanied by high frequency interneurone firing. They are initiated in CA3, spread into the CA1 region of the hippocampus, and pyramidal cell and GABAergic interneurons fire during SPWs of both regions (Csicsvari *et al.* 2000; Klausberger *et al.* 2003). SPWs are suggested to involve various forms of replay of previous sequences of spike discharge and so they have been associated with the consolidation of neuronal representations (Ji & Wilson, 2007; Girardeau *et al.* 2009; Jadhav *et al.* 2012).

SPW-like events occur spontaneously *in vitro* (Kubota *et al.* 2003) and the mechanisms responsible for their generation have mostly been examined in slices. These mechanisms remain controversial and may differ for SPWs of the CA3 and CA1 regions. SPWs have been ascribed to electrotonic junctions between pyramidal cells (Draguhn *et al.* 1998; Böhner *et al.* 2011) or to interactions within recurrent circuits (Ellender *et al.* 2010) with predominant excitatory (Maier *et al.* 2011) or inhibitory synaptic signals (Ho, Zhang & Skinner, 2009; Aivar *et al.* 2014). Data on how single neurones affect the timing or initiation of SPWs could help discriminate between these possible mechanisms. Ellender *et al.* (2010) showed that stimulation of single interneurons increased the probability of SPW occurrence in slices with long (~1 s) latencies, whereas stimulation of single pyramidal cells had no effect.

In the present study, we show, *in vitro*, that firing in single CA3 pyramidal cells could initiate SPW with latencies of 2–6 ms. This latency is similar to that between pyramidal cell firing and the discharge of post-synaptic

interneurons (Miles, 1990; Csicsvari *et al.* 1998). Extracellular records suggested that repeated firing of the same or different interneurons contributed to SPWs. SPWs induced by single cells were more stereotyped than SPWs that occurred spontaneously without stimulation. However, the identities and the timing of interneurone firing varied between successive initiated SPWs.

Methods

Slice preparation

Hippocampal slices were prepared from rats, aged 7–10 weeks and weighing 150–300 g, in accordance with EC Directive 08/120/EC and local INSERM guidelines. Protocols were approved by the Comité d'Ethique Darwin, Ministère de l'Enseignement Supérieur et de la Recherche, Paris. Twenty-two animals were used to obtain the data reported in the present study. Rats were anaesthetized *i.p.* with ketamine (80 mg kg⁻¹) and xylazine (12 mg kg⁻¹) and perfused intracardially with a solution containing (in mM) 62 NaCl, 26 NaHCO₃, 1 KCl, 10 MgCl₂, 1 CaCl₂, 122 sucrose and 10 D-glucose and equilibrated with 5% CO₂ in 95% O₂ at 3–5°C. Both hippocampi were dissected free and transverse slices (thickness 500 μm) were cut with a vibratome (HM650V; Microm International GmbH, Walldorf, Germany) from their ventral portion. Slices were transferred to an interface recording chamber, where they were equilibrated with 5% CO₂ in 95% O₂, heated to 35–37°C and perfused with a solution containing (in mM) 124 NaCl, 26 NaHCO₃, 3–5 KCl, 2 MgCl₂, 2 CaCl₂ and 10 glucose.

Drugs

In some experiments, GABA_A receptor mediated signalling was suppressed by picrotoxin (100 μM). We also used the μ-opioid receptor agonist (D-Ala², N-MePhe⁴, Gly-ol)-enkephalin (20 μM; DAMGO), which is suggested to hyperpolarize perisomatic targeting interneurons and reduce release from inhibitory terminals (Svoboda *et al.* 1999; Gulyas *et al.* 2010). Drugs were obtained from Tocris Neuramin (Bristol, UK) or Ascent Scientific (Cambridge, UK).

Recordings

Intracellular records were made with glass electrodes filled with 4 M KAc (resistance 50–80 MΩ). Signals were amplified with an Axoclamp 2B amplifier (Molecular Devices, Sunnyvale, CA, USA) operated in current-clamp mode. Intracellular records from neurons with overshooting action potentials, an input resistance larger than 20 MΩ and a time constant longer than 10 ms were retained. Extracellular records were made with arrays

of eight to 12 nichrome electrodes (diameter $50\ \mu\text{m}$) positioned to contact slices from above (Bazlot *et al.* 2010). In some experiments, linear arrays with a separation of $\sim 100\ \mu\text{m}$ between electrodes were placed along the CA3 pyramidal cell somatodendritic axis, orthogonal to the stratum pyramidale. In other experiments, curved arrays of separation $\sim 200\ \mu\text{m}$ between electrodes were used to record from sites along the CA3 stratum pyramidale. Signals were amplified and filtered (pass-band 0.1 Hz to 20 kHz) with a 16 channel amplifier (Dr F. Dubois; Dipsi, Châtillon, France). Intracellular and extracellular voltage signals were digitized using a 12 bit, 16 channel analog-to-digital converter (Digidata 1200A; Molecular Devices) and visualized on a PC (Axoscope; Molecular Devices).

Signal analysis

Intracellular and multiple (8–12) extracellular records were analysed with laboratory-written routines (Matlab, MathWorks Inc., Natick, MA, USA; Python, <https://www.python.org>). The amplitude of SPWs and unitary inhibitory synaptic fields (fIPSPs) was measured at their peak on any recording site. Extracellular spikes were detected from signals filtered above 600 Hz using a threshold of $5\times$ the SD of baseline fluctuations. Field IPSPs (fIPSPs) were detected from low pass-filtered (80 Hz) signals as single positive-going waves of amplitude exceeding 5 SDs. SPWs were detected (Fig. 1) from low pass-filtered (80 Hz) signals obtained from eight sites of the CA3 stratum pyramidale. An amplitude threshold was adjusted to detect events similar to user-identified SPWs defined as fields generated at three or more sites, with at least three waves (Fig. 1A).

Wave components of SPWs (Fig. 1B) were detected from zero-crossings of the second derivative of voltage in low-pass filtered records (80 Hz). Spikes associated with SPWs (Fig. 1B) were detected from high-pass filtered traces (600 Hz). The start of an SPW was defined as the shortest latency spikes and/or waves across all recording sites in the stratum pyramidale (Fig. 1C). Sequential wave components of SPWs were defined from their start and peak, as well as the timing of firing, in comparisons of records from all sites in the CA3 stratum pyramidale. An index of the spatial coherence of SPWs, their similarity at different recording sites, was derived as: (summed number of waves detected from all sites)/(the number of recording sites \times number of waves).

Spontaneously occurring and induced fIPSPs and associated spikes were sorted by unsupervised clustering of extracellular signals ($n = 8$) recorded from the stratum pyramidale. Events with overlaps of spikes or fIPSPs were excluded. Traces were measured at multiple time points chosen to provide a good discrimination of extracellular spikes and fIPSPs. The time points, with respect to the

peak of the largest extracellular spike, were typically at -1.0 , -0.5 , 0.1 , 0 (spike peak), 0.1 and 2.0 ms. Subtracting values for each trace from the value at -1.0 ms gave five parameters per trace and with eight channels

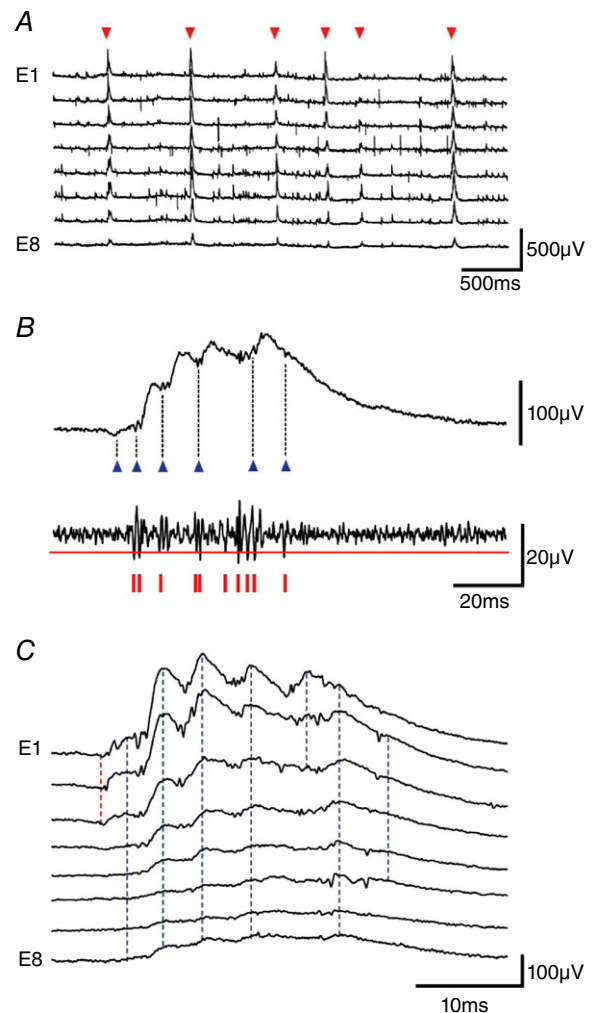


Figure 1. Detection and measurement of SPWs

A, SPWs (red triangles) were recorded extracellularly from the CA3 stratum pyramidale with eight electrodes, E1–E8 separated by $\sim 200\ \mu\text{m}$ in a curved array. SPWs were defined as events recorded from at least three electrodes, comprising three or more waves, and exceeding a user-defined amplitude threshold. B, multi-unit and wave components of SPW fields. Upper trace, SPW field (band pass filtered, 1–80 Hz); lower trace, unit activity (high-pass filtered, 600 Hz). Blue triangles indicate the start of six detected waves and red vertical lines indicate 10 detected spikes. C, SPW recorded by eight extracellular electrodes (E1–E8) from the CA3 stratum pyramidale. The onset of the SPW was detected on electrodes E1–E3 (red dotted line). Seven waves were detected (blue dotted lines). The first, fifth and seventh waves were recorded by some (but not all) electrodes. An index of spatial coherence was used to define the spatial variability of SPWs: (summed number of waves detected from all sites)/(the number of recording sites \times number of waves). The index has a value of 1 for an SPW where each wave is detected at each site. For this event, it was $0.77 = (3 + 8 + 8 + 8 + 3 + 8 + 5)/(8 \times 7)$.

a string of 40 numbers. Strings were analysed using *k*-mean clustering procedures as described previously (Bazelot *et al.* 2010). Reliability of the clustering was confirmed by visual matching of the form of spikes and fIPSPs at all recording sites on sets of eight traces aligned to the peak of the largest extracellular spike. Current source densities were estimated from eight to 12 extracellular records made along the CA3 pyramidal cell somatodendritic axis as described previously (Bazelot *et al.* 2010) using the approximation of Nicholson and Freeman (1975).

Initiated and spontaneous SPWs were selected from all events detected in records with a duration of 10–45 min. SPWs occurring with latencies <5 ms after a pyramidal cell action potential induced by current injection were classed as evoked events. Other SPWs were considered to occur spontaneously. The initiation of spontaneous and evoked SPWs was compared for events aligned at their start, defined from both waves and unit spikes. Extracellular firing at SPW initiation was compared for all spikes detected from all electrodes within 1 ms of the start of the SPW. A cumulative sum procedure was used to compare the variability of spontaneous and single-cell initiated SPWs. A running sum was made from each point, of root-mean-square differences between the voltage trajectory of each event on each electrode, and the mean event from that electrode for all spontaneous or initiated SPWs. Cumulative variability from all electrodes was then added to derive summed values for spontaneous and initiated events. The significance of differences was explored using a bootstrap test, which compared sums of the squared differences from the means of either spontaneous or triggered events with values derived identically from 1000 randomized groups. The amplitude of fIPSPs and SPWs were compared using the peak amplitude detected at any site.

Statistical analysis

Values are reported as the mean \pm SD. Statistical analyses were conducted using Student's *t* test in SigmaStat, version 3.0 (Systat Software Inc., Chicago, IL, USA). $P < 0.05$ was considered statistically significant.

Results

Single pyramidal cells initiate SPWs and field IPSPs

We observed action potentials in some CA3 pyramidal cells affected the timing of SPWs (Fig. 2). Pyramidal cells were made to fire single action potentials by current injection at intervals of 1–5 s. In 10 of 30 CA3b–c pyramidal cells tested, SPWs followed action potentials with latencies of ≤ 5 ms (Fig. 2A–C) and a probability of 0.07–0.76 (from 250 or

more trials). The probability of SPW occurrence by chance was estimated to be in the range 0.002–0.012, as a result of dividing the latency of 5 ms by the mean interval between SPWs for each slice (Prida *et al.* 2006). The mean delay from the pyramidal cell spike to the first wave of the SPW was 2.7 ± 0.5 ms (20% of peak; $n = 10$) (Fig. 2B and C). Initiated SPWs were accompanied by an increase in multi-unit activity. The duration and pattern of this firing is shown in Fig. 2D, which plots all the extracellular spikes from SPWs initiated by single pyramidal cells ($n = 10$ cells; 38–252 SPWs per cell).

A delay of 2–3 ms is similar to that between pyramidal cell firing and discharge of a post-synaptic interneurone (Miles, 1990; Csicsvari *et al.* 1998). Field IPSPs are an extracellular sign of the activation of all the inhibitory synapses established by a single interneurone (Glickfeld *et al.* 2009; Bazelot *et al.* 2010). We found the same pyramidal cells induced either SPWs (Fig. 2E) or fIPSPs (Fig. 2F) with similar latency. Both fIPSPs and SPWs could be preceded by an extracellular action potential typically of short duration (0.3–0.6 ms; $n = 10$) as associated with interneurone firing (Henze *et al.* 2000). The probability of inducing a fIPSP was 0.08–0.42 ($n = 10$ cells; 250 or more trials). The observation that a single pyramidal cell could initiate either a fIPSP or a SPW suggested that the same circuits might be involved. Similar latencies (Fig. 2E and F) and spike shapes (Fig. 2G) suggest that the same extracellular unit may have fired when a single pyramidal cell initiated a fIPSP or a SPW.

fIPSPs from perisomatic interneurons are repeated in SPW fields

We therefore examined the role of interneurons and inhibitory synaptic circuits in SPW generation. Most recorded pyramidal cells were inhibited both during spontaneous SPWs and those that they initiated (24 of 30 neurons) (Figs 2B and 3A). Three were depolarized and three others received mixed excitatory–inhibitory synaptic events (not shown). Inhibitory events occurring during a SPW were correlated in time and in amplitude with fields recorded from the stratum pyramidale. By contrast, all ($n = 4$) fast-spiking interneurons recorded close to the stratum pyramidale received depolarizing events correlated with successive waves of SPWs (Fig. 3B)

There was a continuum between single inhibitory events and multi-component SPWs in field records and intracellular traces from pyramidal cells. Each wave of a SPW field was similar in form to a fIPSP of time to peak 2–5 ms (Glickfeld *et al.* 2009; Bazelot *et al.* 2010). Typically, three to 10 waves were repeated at intervals of 4–10 ms. Figure 3C shows a superimposition of field and pyramidal cell membrane potential records for an isolated fIPSP and SPWs of up to four waves. Figure 3D shows that, although

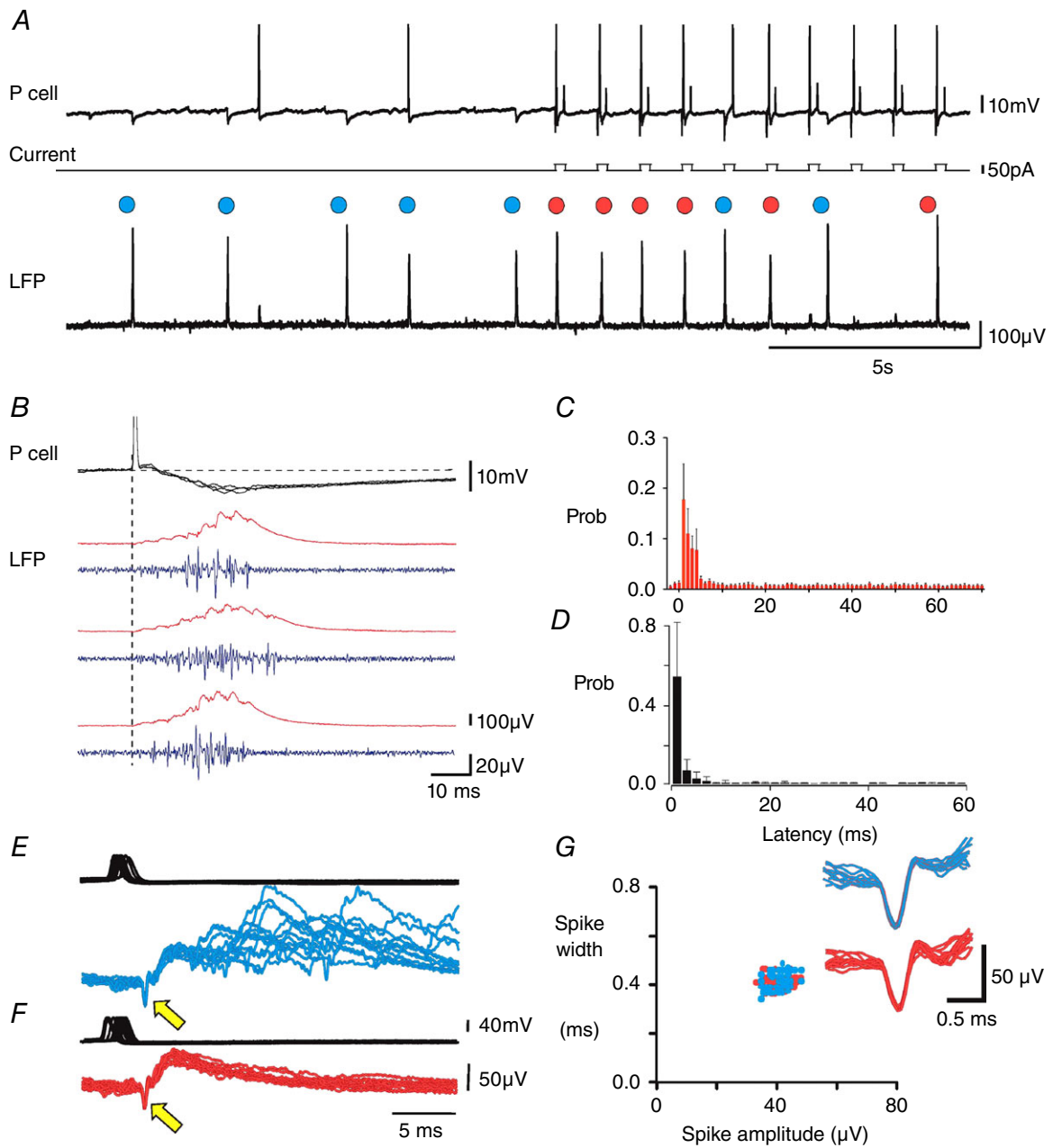


Figure 2. Single CA3 pyramidal cells trigger SPWs

A, traces are CA3 pyramidal cell membrane potential, injected current and local field potential (LFP). Blue circles indicate spontaneously occurring SPWs at intervals of 1.5–3.0 s. Current pulses (50 pA, duration 200 ms, interval 1000 ms) were injected to induce single pyramidal cell action potentials almost half-way along the traces. Red circles indicate six of 10 action potentials followed at short latency by a SPW. Overall, 172 of 626 spikes induced in this pyramidal cell were followed by a SPW at a latency shorter than 5 ms. In total, 99 spikes elicited no response, 128 spikes evoked a single fIPSP and 227 spikes elicited events intermediate between a single fIPSP and an SPW. *B*, three SPWs initiated by pyramidal cell firing. Intracellular potential, field (red) and multi-unit firing (blue, 0.5–5 kHz band-pass filtered). *C*, interval distribution between the intracellular action potential and the start of detected SPWs ($n = 10$ experiments, 1145 SPWs, mean \pm SD of probabilities). *D*, normalized probability distribution of latencies from single pyramidal action potentials to extracellular spikes associated with the next SPW (mean \pm SD of probabilities, $n = 1726$ action potentials from 10 pyramidal cells). *E–G*, SPWs, fIPSPs and unit firing. *E*, overlay of 20 SPWs (blue) initiated by single pyramidal cell action potentials (upper trace) and preceded by an extracellular spike (yellow arrow). *F*, overlay of 20 fIPSPs (red), initiated by single pyramidal cell spikes (upper trace) and preceded by an extracellular spike (yellow arrow). Traces of (*E*) and (*F*) triggered on the extracellular spike. *G*, plot of width against amplitude for spikes preceding fIPSPs (red) and SPWs (blue). The inset shows overlays of extracellular spikes preceding SPWs ($n = 20$, blue) and fIPSPs ($n = 20$, red).

one interneurone action potential evoked a fIPSP, repeated firing elicited field events similar to those at the start of a SPW. Relationships between peak field amplitude and the amplitude of depolarizations in interneurons ($n = 4$) or hyperpolarizations in pyramidal cells ($n = 8$) are summarized in Fig. 3E ($n = 300$ – 800 events at resting potential). Peak SPW field amplitude and membrane hyperpolarizations in pyramidal cells increased together with the number of waves in a SPW (Fig. 3F). Figure 3G shows how the spatial coherence of SPWs (see Methods) recorded from multiple electrodes also co-varied with field amplitude and the number of waves. These data suggest that a continuum exists between fIPSPs consisting of a single wave and SPWs of up to eight to 10 waves.

We next attempted to compare the identity of inhibitory synapses contributing to fIPSPs and to SPWs using current source density analysis. Fields were recorded with multiple electrodes ($n = 12$) from sites along the somatodendritic axis of CA3 pyramidal cells ($n = 5$ slices). Comparisons of the spatial profiles of fIPSPs (Fig. 4A) and an intermediate wave of SPWs (Fig. 4B) revealed a current source in the stratum pyramidale. These data suggest that pyramidal cells initiating SPWs also excite interneurons (Csicsvari *et al.* 1998). Repeated firing in the same or different interneurons is associated with succeeding waves of the SPW field.

Confirmation that interneurons are involved in SPW generation was obtained by showing that SPWs were

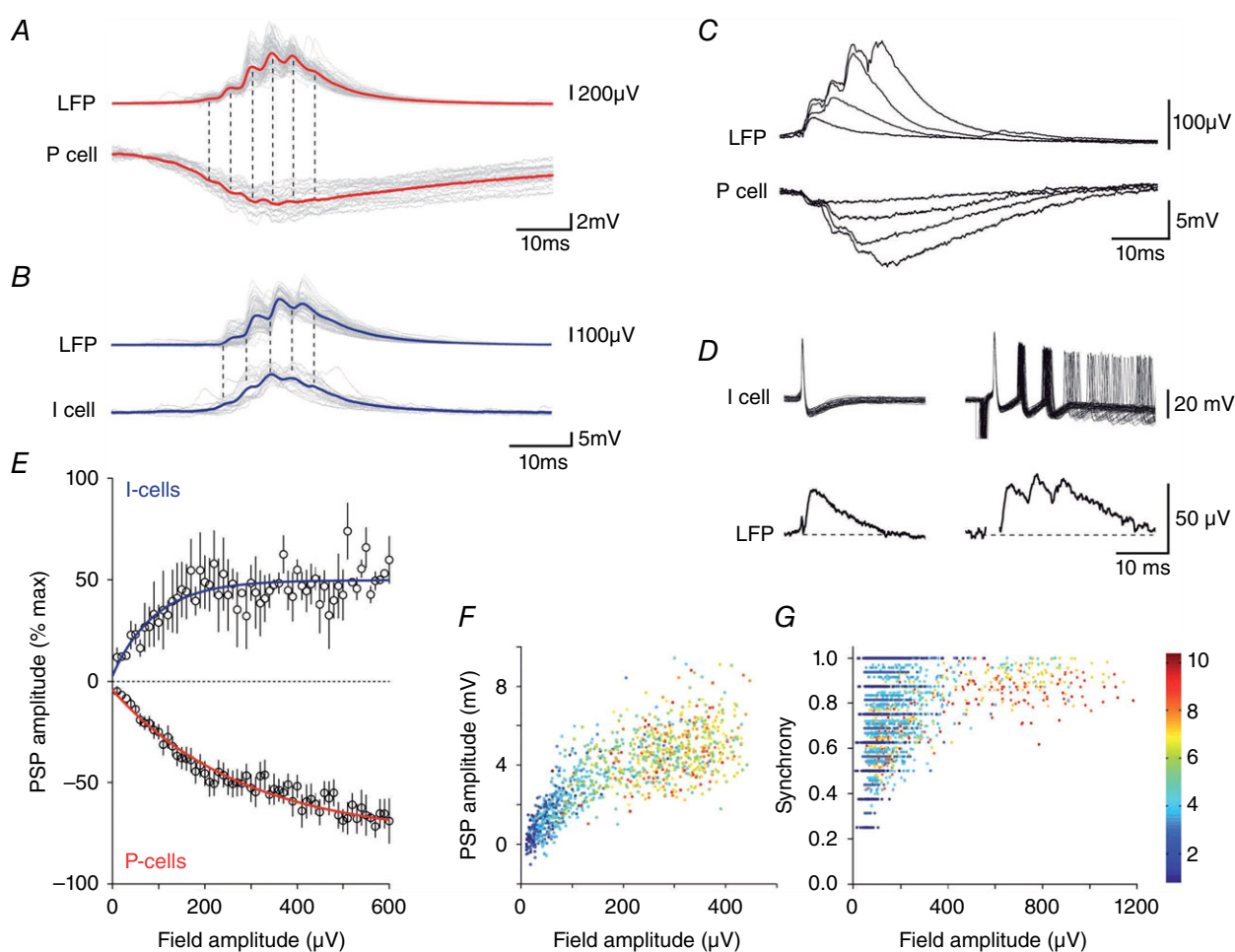


Figure 3. Synaptic events corresponding to SPWs and fIPSPs

Correlates of SPWs in pyramidal cells (red) (A) and in interneurons (blue) (B) showing the averaged local field and intracellular membrane potential with overlays of 20 traces (grey). C, overlaid field and pyramidal cell membrane potentials for a fIPSP and for SPWs of up to four waves; same records as in (A). D, field potentials (average of 30) induced by single and multiple action potentials in an interneurone. E, peak SPW field amplitude plotted against membrane potential changes in interneurons (blue, $n = 4$, $r^2 = 0.22$) and pyramidal cells (red, $n = 16$, $r^2 = 0.96$). F, hyperpolarizing change in pyramidal cell membrane potential ($n = 16$) plotted against the amplitude of fields associated with events from single fIPSPs (blue) to eight to 10 wave SPWs (red). G, spatial coherence for fIPSPs (blue) through to eight to 10 wave SPWs (red) plotted against field potential amplitude (all events from 10 slices).

suppressed by the GABA_A receptor antagonist picrotoxin ($20 \mu\text{M}$; $n = 5$, data not shown). The opiate DAMGO, which hyperpolarizes and reduces transmitter release from perisomatic interneurons (Svoboda *et al.* 1999; Gulyas *et al.* 2010), also suppressed SPWs ($20 \mu\text{M}$, $n = 4$) (Fig. 4C and D). Together with the current profile data (Fig. 4A and B), these data suggest that interneurons forming perisomatic synapses contribute to SPW fields. Pyramidal cell initiation of SPWs involves the excitation of one or several perisomatic interneurons.

Excitation of interneurons by single pyramidal cells

We estimated the number and spatial distribution of interneurons discharged by single pyramidal cells by making multiple extracellular records of fIPSPs from sites along the CA3 stratum pyramidale with eight electrodes separated by $\sim 200 \mu\text{m}$ (Fig. 5). Inhibitory fields were typically recorded from three to six of these electrodes (Fig. 5A–D), which is consistent with the dimensions of axonal arbors of perisomatically-terminating inhibitory cells in this region (Gulyas *et al.* 2010). fIPSPs were often preceded, at two to four recording sites, by a short-duration extracellular spike (Figs 2E and F and 5A–D). These two features, a local spike, presumably generated by an interneurone, and a more

widespread fIPSP of distinct amplitude distribution across different sites, could define multiple, spatially different inhibitory field motifs.

Pyramidal cells that initiated SPWs also activated multiple distinct fIPSP motifs. Overlays of traces selected after clustering and template matching show (Fig. 5A–D) that a single pyramidal cell initiated distinct fIPSPs with maximal amplitude at different recording sites preceded by a short-duration extracellular spike. Nine of 10 single pyramidal cells that initiated SPWs (Fig. 2) initiated at least two (2–6) spatially distinct fIPSP motifs. The other initiating cell evoked fIPSPs, although no extracellular spike was reliably detected. Plotting distances between stimulated pyramidal cells ($n = 10$) and all detected spikes (31 spikes of amplitude larger than $20 \mu\text{V}$) revealed a distribution clustered around the initiating neurone (Fig. 5E). Extracellular spikes preceding fIPSPs were typically recorded on several electrodes (Fig. 5F). This is unexpected because the amplitude of extracellular spikes generated by pyramidal cells decays to undetectable levels at distances of $\sim 100 \mu\text{m}$ (Cohen & Miles, 2000; Henze *et al.* 2000). The extracellular spike shown in Fig. 5F, propagated at $\sim 1 \text{ mm ms}^{-1}$, which is similar to the speed of action potential conduction in interneurone axons (Hu & Jonas, 2014).

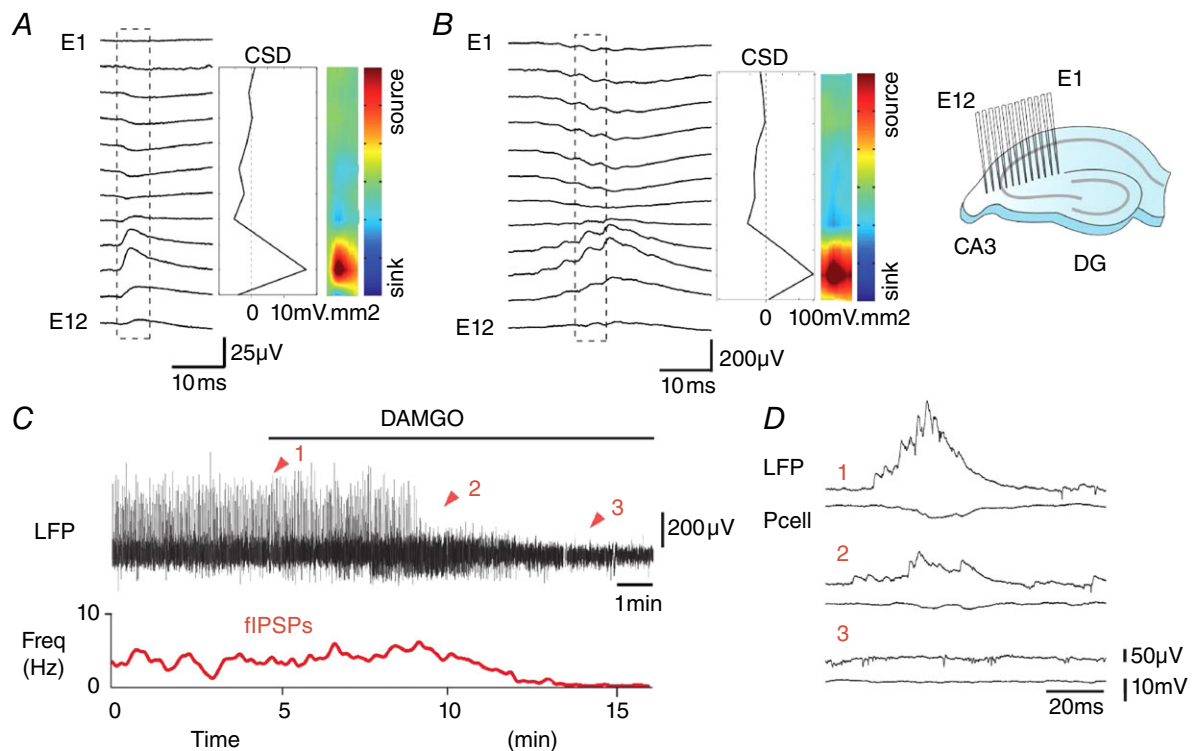


Figure 4. Evidence for activation of perisomatic inhibitory synapses during SPWs

Comparison of CSD profiles for a fIPSP (A) and an intermediate wave of a SPW (B) recorded with 12 electrodes (E1–E12, separation $\sim 100 \mu\text{m}$) placed along the CA3 pyramidal cell somatodendritic axis (inset). A current source (red) was apparent near the stratum pyramidale for both fIPSPs ($n = 200$) and SPWs ($n = 200$). C and D, DAMGO ($20 \mu\text{M}$) suppressed both SPWs and fIPSPs. Traces are the LFP (upper) and fIPSP frequency (red, lower). D, field and pyramidal cell potentials during DAMGO application as indicated by red arrows (1–3).

Comparison of spontaneous SPWs and SPWs initiated by single cells

If pyramidal cells tend to discharge nearby interneurons, then evoked SPWs might also be initiated at sites clustered around a stimulated pyramidal cell. We examined this by comparing initiation sites for initiated and spontaneously occurring SPW field potentials in the stratum pyramidale. The initial wave of initiated SPW fields always began close to the initiating cell (Fig. 6A and C). By contrast, spontaneous SPWs were typically initiated at multiple sites in CA3 (Fig. 6B and C). Thus, although SPWs appear to be initiated via the firing of interneurons near the stimulated

pyramidal cell, spontaneous SPWs may depend on similar processes at multiple, distinct sites.

We compared several characteristics of spontaneous SPWs and those initiated by single pyramidal cells. The duration of SPWs was measured as the delay between the start of the first and the last detected fIPSP. For initiated events, the mean duration was 23.8 ± 5.3 ms and, for spontaneous events, it was 21.6 ± 4.0 ms (paired *t* test, $P = 0.15$, $n = 1233$ initiated and 1233 spontaneous events from 10 different slices). The mean number of waves or fIPSPs was counted across eight recording sites, with events simultaneous at multiple sites counted as one event. There were 6.7 ± 1.4 waves for initiated events and

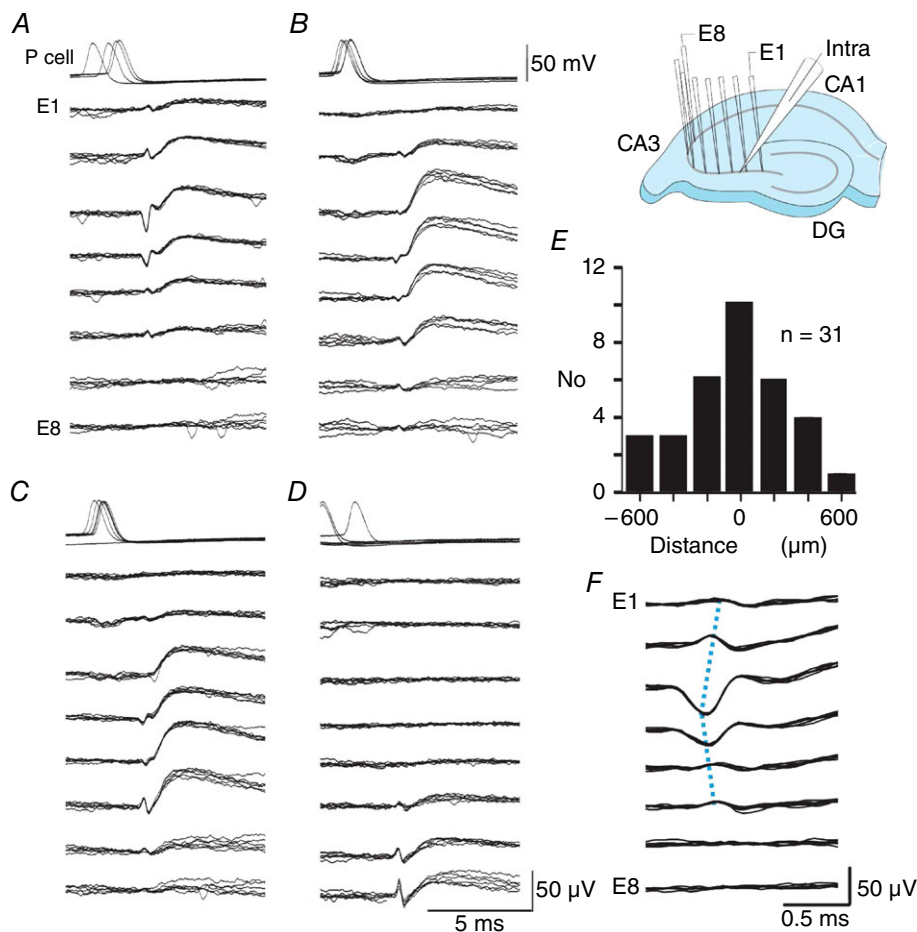


Figure 5. Single pyramidal cells induce firing in multiple interneurons

A to D, single action potentials of the same CA3 pyramidal cell initiated four spatially distinct combinations of an extracellular spike followed by a field IPSP. Overlays of six traces for pyramidal cell potential and extracellular potentials at eight sites in the stratum pyramidale (inset, E1–E8, electrode separation 200 μm). All sets of traces are aligned on the largest extracellular spike. Spikes were detected at three to six sites and fIPSPs were recorded by three to seven electrodes. In total, 436 action potentials of this pyramidal cell triggered 90 fIPSPs, 130 events intermediate between fIPSPs and SPWs, and 178 SPWs, and 38 spikes elicited no response. A, the largest spike amplitude was ~ 55 μV on E3 (13 of 90 initiated fIPSPs). B, the largest spike was ~ 25 μV on E4 (18 of 90 fIPSPs). C, the largest spike was ~ 40 μV on E6 (43 of 90 fIPSPs). D, the largest spike amplitude was ~ 55 μV on E8, (16 of 90 fIPSPs). E, distance between the initiating pyramidal cell and the site of the maximal extracellular spike ($n = 31$ spikes of amplitude > 20 μV; duration < 0.6 ms, initiated by 10 pyramidal cells). F, enlarged extracellular spikes from (A), detected over distances of 4–800 μm, suggest that interneurone axonal action potentials may propagate at ~ 1 mm ms⁻¹ (blue dotted lines aligned to spike peaks).

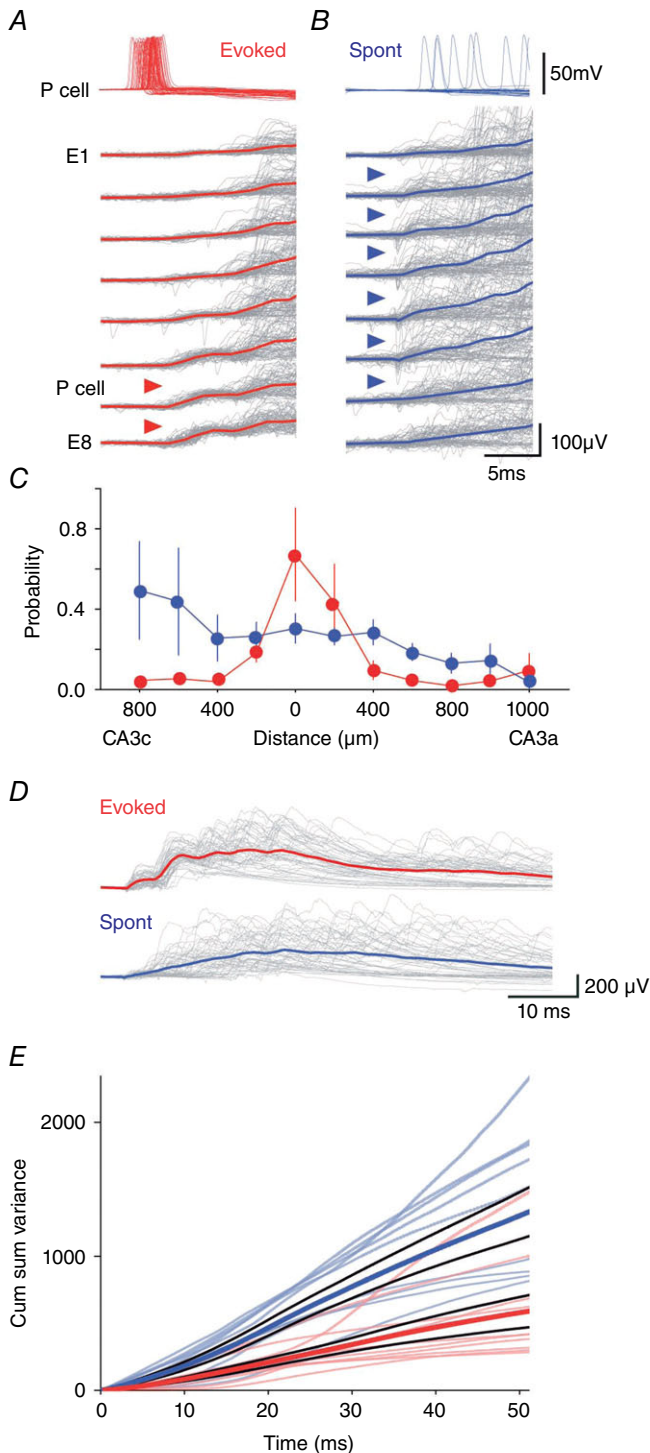


Figure 6. Differences between initiated and spontaneous SPW fields

The site of initiation for evoked SPWs (red triangles) (*A*) varied less than that of spontaneous SPWs (blue triangles) (*B*). Overlay (grey) and averages of 100 initiated (red) and 100 spontaneous SPWs recorded over the same period from electrodes E1–E8 in the CA3 stratum pyramidale. SPWs were aligned at their initiation site defined from spikes and field. The stimulated pyramidal cell was situated between E6 and E7. *C*, the spatial distribution of extracellular unit

6.3 ± 1.2 waves for spontaneous events (paired *t* test, $P = 0.29$, $n = 2466$). The mean interval between fIPSPs, from all electrodes, was 6.7 ± 1.4 for initiated events and 7.1 ± 1.0 for spontaneous events (paired *t* test, $P = 0.17$, $n = 2466$). On the basis of these criteria, initiated events did not differ from spontaneously occurring SPWs.

Finally, we investigated whether later phases of initiated SPW fields followed a more stereotyped time course than spontaneous SPW fields (Fig. 6*D*). As an index of field variability, we used a cumulative sum of root-mean-square differences between each field potential and the mean field from each electrode (see Methods). Identical numbers of initiated and spontaneous SPWs from the same time period for each recording were analysed ($n = 10$). This index of cumulative field variability was always lower near the start of initiated SPWs, as expected, because the initiation site tended to be more stereotyped. Figure 6*D* and *E* shows that the lower variability for initiated SPWs was maintained throughout their time course. If SPW fields in the stratum pyramidale largely reflect fIPSPs, then the set of interneurons firing during evoked SPWs may be more stereotyped than those active during spontaneous SPWs.

Patterns of SPW spread and the activity of identified interneurons

We attempted to identify interneurons that fired during SPWs from the involvement of distinct spike and fIPSP motifs in SPW fields. We searched for spatially distinct events involving large extracellular spikes ($>20 \mu\text{V}$) as shown in Fig. 5. In seven of 10 records, we could distinguish (1) a motif triggered by a pyramidal cell that initiated SPWs and (2) a second inhibitory motif not evoked by that pyramidal cell. Figure 7*A* shows an example where the initiated motif consisted of a maximal spike on electrode E3 and a fIPSP on electrodes E1–E6. By contrast, the inhibitory motif shown in Fig. 7*B*, consisting of a maximal spike on electrode E6 and a fIPSP on electrodes E3–E8, was not initiated by the recorded pyramidal cell.

Both extracellular units (Fig. 7*A* and *C*) appeared to participate in initiated SPWs (Fig. 7*C*–*E*). Isolated motifs and those embedded in SPWs were compared on the basis of spike amplitude and shape, as well as on the amplitude

activity at the start of initiated SPWs (red) was more restricted than that preceding spontaneous events (blue). Data from 10 slices, with distance $0 \mu\text{m}$ corresponding to the extracellular electrode closest to the initiating cell. *D*, cumulative variability of SPW fields was less for initiated than spontaneous events ($P = 0.016$, bootstrap). Above: overlays of 50 evoked SPWs (grey, mean shown in red) and 50 spontaneous SPWs (grey, mean shown in blue). *E*, time course of cumulative variability for initiated (red, $n = 10$ slices) and spontaneous SPWs (blue; $n = 10$), with mean \pm SE (bold lines). A lower variability at initiation was maintained through SPW time course.

and form of fIPSPs recorded from all electrodes. In this way, the initiated motif of Fig. 7A appeared to be involved in 81 of 118 (69%) and the non-initiated fIPSP motif of Fig. 7B in 37 of 118 (31%) of triggered SPWs. FIPSP motifs triggered by initiating pyramidal cells were detected in SPWs with probabilities of 38–82% ($n = 7$). Identified fIPSP motifs that were not elicited by pyramidal cell firing were detected with probability of 16–62% ($n = 7$). These data suggest that, as SPWs spread, previously silent interneurons were recruited at longer latencies than directly excited interneurons. The occurrence and the timing of firing in identified interneurons during SPWs initiated by the same pyramidal cell varied between trials (Fig. 6).

Discussion

Single identified neurons of invertebrates and fish can initiate motor behaviours (Ikeda & Wiersma, 1964; Getting & Deakin 1985; Eaton, Bombardieri & Mayer, 1977). Single mammalian pyramidal cells can affect movement (Brecht *et al.* 2004), sensory perception

(Houweling & Brecht, 2008), volition (Fried, Mukamel & Kreiman, 2011), entrain or initiate population activities (Miles & Wong, 1983; Prida *et al.* 2006; Bonifazi *et al.* 2009), and alter EEG activities between patterns associated with different brain states (Li, Poo & Dan, 2009). These effects depend on the identity and numbers of neurons driven to discharge by firing in the single initiating cell (Kwan & Dan, 2012).

Data are reported in the present study showing that ~30% of CA3 pyramidal cells triggered SPW-like events *in vitro*. We further show that these pyramidal cells evoked firing at similar latencies in several (2–6) perisomatic interneurons. Comparison of inhibitory fields and SPW fields suggested that, during a SPW, different interneurons fire repeatedly at intervals of 3–8 ms.

Advantages of an *in vitro* study

The work in the present study was facilitated by employing an *in vitro* approach. Accurate placement of linear electrode arrays orthogonal to the CA3 stratum pyramidale permitted field profile analyses of current profiles associated with SPWs and fIPSPs. Curved arrays

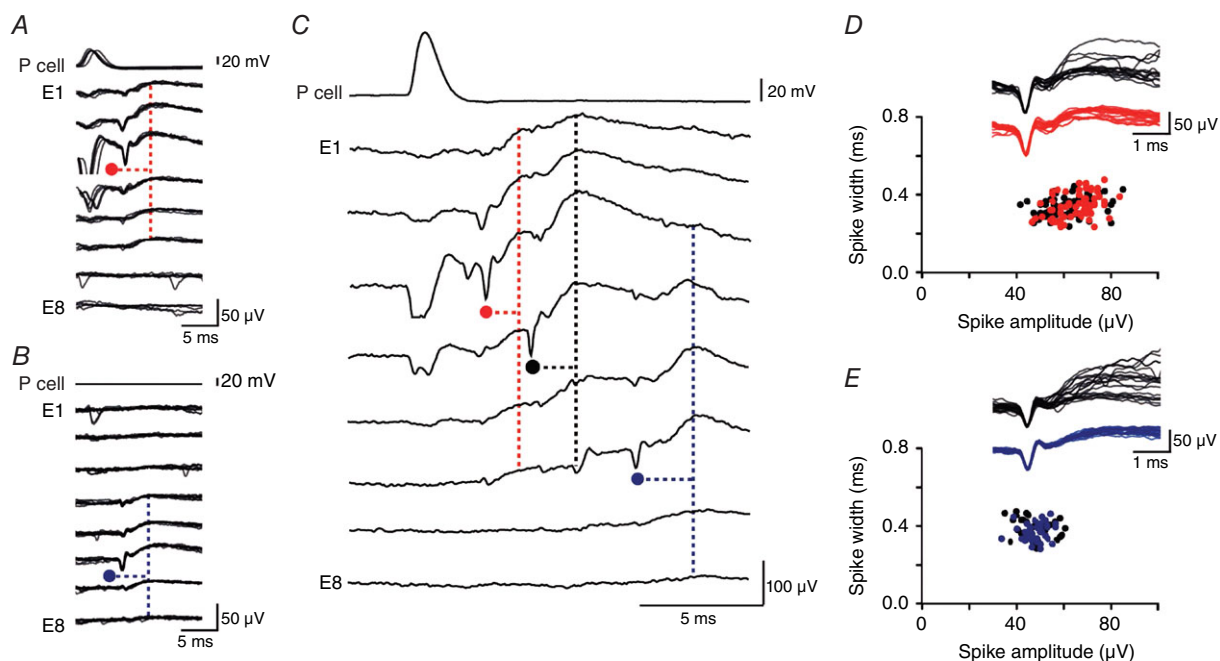


Figure 7. Field inhibitory motifs during SPWs

A, pyramidal cell spikes induce a presumed interneurone spike (red, maximum on electrode E3) and associated fIPSP. In total, 377 pyramidal cell action potentials initiated 130 single fIPSPs and 118 SPWs. Traces aligned on the extracellular spike. B, a spatially distinct interneurone spike (blue, maximum on E6) and fIPSP was never initiated by pyramidal cell firing. A and B, pyramidal cell and eight extracellular records from the stratum pyramidale. C, spike and fIPSP motifs were evident during SPWs initiated by the stimulated pyramidal cell. One interneurone spike (red, E3; A) occurs at ~2 ms and the other (blue, E6; B) at ~10 ms after pyramidal cell firing in this example. Another putative interneurone spike of amplitude >20 μV (black, maximum on E4) occurs at a latency of ~5 ms. D, amplitude plotted against width of spikes initiated by the pyramidal cell and recorded by electrode E3 before fIPSPs (red) or SPWs (black). Examples are overlain in the inset (fIPSPs, $n = 20$, red; SPWs, $n = 20$, black). E, amplitude plotted against width for spikes not directly initiated by the pyramidal cell and recorded on electrode E6 before fIPSPs (blue) or SPWs (black). Overlaid examples in the insets (fIPSPs, $n = 20$, blue; SPWs, $n = 20$, black).

placed along the stratum pyramidale allowed us to discriminate between the firing of different interneurons and the fIPSPs that they generated, revealing distinct fIPSP motifs. SPW-like fields *in vitro* have a form and duration similar to those recorded in the intact animal. Equally, single pyramidal cells discharge post-synaptic interneurons at comparable latencies and probabilities *in vivo* (Csicsvari *et al.* 1998), as well as in slices kept in an interface chamber (Miles, 1990). Inhibitory field motifs consisting of an interneurone spike followed mono-synaptically by a spatially extended fIPSP have not yet been detected *in vivo*, possibly as a result of higher levels of background field fluctuations. Lower levels of fluctuation in fields in slices may have facilitated attempts to follow the firing of specific interneurons during SPWs.

We used a clustering approach to sort inhibitory motifs identified by measurements of spike and inhibitory field waveforms, followed by visual comparison of aligned traces. To validate this approach, multiple field records from stratum pyramidale could be compared with responses to single action potentials of intracellularly recorded, anatomically identified interneurons (Bazelot *et al.* 2010). This would provide data on the variability and spatial distribution of extracellular spikes and inhibitory fields initiated by an identified interneuron and also permit comparison with other extracellularly recorded motifs.

Population activities involving interneurons may be detected more easily when slices are maintained at a liquid–gas interface or when precautions are taken to enhance oxygenation of submerged slices (Hajos *et al.* 2009). The amplitude of field IPSPs recorded from slices in interface chambers is several times larger than similar events recorded from submerged slices (Glickfeld *et al.* 2009; Bazelot *et al.* 2010). These factors may have contributed to the data reported by Ellender *et al.* (2010) suggesting that single pyramidal cell firing does not influence SPWs in submerged slices.

Initiating pyramidal cells excite perisomatic interneurons

Evidence suggesting that SPW initiation involves pyramidal cell excitation of interneurons (Figs 5 and 7) is based on the latency of initiated events and signs of interneurone firing at the start of SPWs (Hajos *et al.* 2013; Sasaki, Matsuki & Ikegaya, 2014; Schlingloff *et al.* 2014). The intervals between pyramidal cell firing and SPW initiation are comparable to the delays between pyramidal cell firing and spikes discharged by a post-synaptic interneurone. By contrast, transmission of firing between mono-synaptically coupled pyramidal cells requires multiple pre-synaptic action potentials and occurs at latencies of 10–15 ms or more (Miles & Wong, 1987; Kwan & Dan, 2012; Ikegaya *et al.* 2013).

Extracellular spikes detected at SPW initiation possessed characteristics of interneurone spikes (Henze *et al.* 2000). When SPWs were not triggered, these spikes could be followed by unitary extracellular inhibitory fields (Glickfeld *et al.* 2009; Bazelot *et al.* 2010). Recorded from the stratum pyramidale, SPW fields apparently correspond to repeated, summed fIPSPs at intervals of 3–8 ms, as first suggested by Buzsáki *et al.* (1992). Our comparison of current sources for fIPSPs and SPWs, as well as the suppression of SPWs by the opiate DAMGO, suggests that the interneurons involved synapse with pyramidal cells at perisynaptic sites as inferred from studies performed *in vitro* (Hajos *et al.* 2013; Aivar *et al.* 2014) and *in vivo* (Klausberger *et al.* 2003).

Continuation, spread and cellular components of SPWs

Although our data suggest that interneurone firing, which may be induced by pyramidal cells, should precede SPWs, they do not clarify the mechanisms ensuring repeated firing of the same or different interneurons as SPWs continue. Records from interneurons (Fig. 3B) show repeated, fast depolarizations aligned with each wave of a SPW. Possibly, these events reflect excitatory synaptic inputs from pyramidal cells. However, few pyramidal cells fired during SPW-like events and the second EPSP in interneurons appears to occur too soon (at 5–10 ms after SPW initiation) for it to depend on synaptically induced firing in pyramidal cells recruited by the initiating cell. Figure 5 shows that single initiating pyramidal cells can induce firing in multiple interneurons. Firing is probabilistic. Not all innervated interneurons fire in response to the same pyramidal cell action potential, and we found no evidence for a delayed firing by different interneurons that could sculpt successive waves of a SPW (Sasaki *et al.* 2014). Possibly, interactions between interneurons (Fukuda & Kosaka, 2000) ensure that SPWs continue after their initiation. If so, such interactions should be able to generate the repeated depolarizations recorded from interneurons during a SPW (Fig. 3B). Alternatively repeated events emerging from supralinear dendritic electrogenesis may ensure that SPWs continue (Memmesheimer, 2010).

Records with electrodes placed along the CA3 stratum pyramidale demonstrate how SPW-like events spread in a slice. SPWs are known to propagate from CA3 into the CA1 region (Csicsvari *et al.* 2000; Maier, Nimrich & Draguhn, 2003) and macroscopic array records show that some SPWs are spatially restricted in the intact animal, whereas others spread longitudinally throughout the CA3 region (Patel *et al.* 2013). At the smaller scale of a transverse slice, our data suggest that previously silent, distant interneurons fire as later waves of a SPW field spread to new sites. Because these interneurons are not excited by the initiating pyramidal cell (Fig. 7),

they must be recruited in another way. Their activity generates a spatially distinct fIPSP and so underlies, in part, propagation of the SWP field.

Field potentials of SPWs initiated by single pyramidal cells are more stereotyped than those associated with spontaneous SPWs (Fig. 6A and D). However, even if only some participating neurones were recognized, our data show variation with respect to the occurrence and identity of directly triggered interneurone firing and those of interneurones indirectly recruited during the later stages of SPWs (Figs 2, 5 and 7). Presumably, more complex mechanisms control the apparently precise time sequences of pyramidal cell firing replay during SPWs in the intact animal (Lee & Wilson, 2002; Diba & Buzsáki, 2007; Stark *et al.* 2014).

In summary, the results of the present study reveal a continuum between single fIPSPs and SPWs. Both events were triggered by some (~30%) recorded pyramidal cells. Latencies were consistent with those for the transmission of firing at synapses that excite interneurones. Multiple extracellular records allow us to separate spatially distinct spikes of interneurones and the resulting inhibitory fields. In this way, pyramidal cells that initiate SPWs were shown to excite several interneurones. The identification of different interneurones and the fields that they produced revealed (1) fluctuations in the composition of SPWs initiated by the same pyramidal cell and (2) the recruitment of previously silent inhibitory cells as SPWs spread through the CA3 region.

References

- Aivar P, Valero M, Bellistri E & Prida LM (2014). Extracellular calcium controls the expression of two different forms of ripple-like hippocampal oscillations. *J Neurosci* **34**, 2989–3004.
- Bähner F, Weiss EK, Birke G, Maier N, Schmitz D, Rudolph U, Frotscher M, Traub RD, Both M & Draguhn A (2011). Cellular correlate of assembly formation in oscillating hippocampal networks in vitro. *Proc Natl Acad Sci USA* **108**, E607–E616.
- Bazelot M, Dinocourt C, Cohen I & Miles R (2010). Unitary inhibitory field potentials in the CA3 region of rat hippocampus. *J Physiol* **588**, 2077–2090.
- Bonifazi P, Goldin M, Picardo MA, Jorquera I, Cattani A, Bianconi G, Represa A, Ben-Ari Y & Cossart R (2009). GABAergic hub neurons orchestrate synchrony in developing hippocampal networks. *Science* **326**, 1419–1424.
- Brecht M, Schneider M, Sakmann B & Margrie TW (2004). Whisker movements evoked by stimulation of single pyramidal cells in rat motor cortex. *Nature* **427**, 704–710.
- Buzsáki G, Leung LW & Vanderwolf CH (1983). Cellular bases of hippocampal EEG in the behaving rat. *Brain Res* **287**, 139–171.
- Buzsáki G, Horváth Z, Urioste R, Hetke J & Wise K (1992). High-frequency network oscillation in the hippocampus. *Science* **256**, 1025–1027.
- Cohen I & Miles R (2000). Contributions of intrinsic and synaptic activities to the generation of neuronal discharges in in vitro hippocampus. *J Physiol* **524**, 485–502.
- Csicsvari J, Hirase H, Czurko A & Buzsáki G (1998). Reliability and state dependence of pyramidal cell-interneuron synapses in the hippocampus: an ensemble approach in the behaving rat. *Neuron* **21**, 179–189.
- Csicsvari J, Hirase H, Mamiya A & Buzsáki G (2000). Ensemble patterns of hippocampal CA3-CA1 neurons during sharp wave-associated population events. *Neuron* **28**, 585–594.
- Diba K & Buzsáki G (2007). Forward and reverse hippocampal place-cell sequences during ripples. *Nat Neurosci* **10**, 1241–1242.
- Draguhn A, Traub RD, Schmitz D & Jefferys JG (1998). Electrical coupling underlies high-frequency oscillations in the hippocampus in vitro. *Nature* **394**, 189–192.
- Eaton RC, Bombardieri RA & Meyer DL (1977). The Mauthner-initiated startle response in teleost fish. *J Exp Biol* **66**, 65–81.
- Ellender TJ, Nissen W, Colgin LL, Mann EO & Paulsen O (2010). Priming of hippocampal population bursts by individual perisomatic-targeting interneurons. *J Neurosci* **30**, 5979–5991.
- Fried I, Mukamel R & Kreiman G (2011). Internally generated preactivation of single neurons in human medial frontal cortex predicts volition. *Neuron* **69**, 548–562.
- Fukuda T & Kosaka T (2000). Gap junctions linking the dendritic network of GABAergic interneurons in the hippocampus. *J Neurosci* **20**, 1519–1528.
- Getting PA & Dekin MS (1985). Mechanisms of pattern generation underlying swimming in *Tritonia*. IV. Gating of central pattern generator. *J Neurophysiol* **53**, 466–480.
- Girardeau G, Benchenane K, Wiener SI, Buzsáki G & Zugaro MB (2009). Selective suppression of hippocampal ripples impairs spatial memory. *Nat Neurosci* **12**, 1222–1223.
- Glickfeld LL, Roberts JD, Somogyi P & Scanziani M (2009). Interneurons hyperpolarize pyramidal cells along their entire somatodendritic axis. *Nat Neurosci* **12**, 21–23.
- Gulyás AI, Szabó GG, Ulbert I, Holderith N, Monyer H, Erdélyi F, Szabó G, Freund TF & Hájos N (2010). Parvalbumin-containing fast-spiking basket cells generate the field potential oscillations induced by cholinergic receptor activation in the hippocampus. *J Neurosci* **30**, 15134–15145.
- Hájos N, Ellender TJ, Zemankovics R, Mann EO, Exley R, Cragg SJ, Freund TF & Paulsen O (2009). Maintaining network activity in submerged hippocampal slices: importance of oxygen supply. *Eur J Neurosci* **29**, 319–327.
- Hájos N, Karlócai MR, Németh B, Ulbert I, Monyer H, Szabó G, Erdélyi F, Freund TF & Gulyás AI (2013). Input-output features of anatomically identified CA3 neurons during hippocampal sharp wave/ripple oscillation in vitro. *J Neurosci* **33**, 11677–11691.
- Henze DA, Borhegyi Z, Csicsvari J, Mamiya A, Harris KD & Buzsáki G (2000). Intracellular features predicted by extracellular recordings in the hippocampus in vivo. *J Neurophysiol* **84**, 390–400.
- Ho EC, Zhang L & Skinner FK (2009). Inhibition dominates in shaping spontaneous CA3 hippocampal network activities in vitro. *Hippocampus* **19**, 152–165.

- Houweling AR & Brecht M (2008). Behavioural report of single neuron stimulation in somatosensory cortex. *Nature* **451**, 65–68.
- Hu H & Jonas P (2014). A supercritical density of Na⁺ channels ensures fast signalling in GABAergic interneuron axons. *Nat Neurosci* **17**, 686–693.
- Ikeda K & Wiersma CAG (1964). Autogenic rhythmicity in the abdominal ganglia of the crayfish: the control of swimmeret movements. *Comp Biochem Physiol* **12**, 107–115.
- Ikegaya Y, Sasaki T, Ishikawa D, Honma N, Tao K, Takahashi N, Minamisawa G, Ujita S & Matsuki N (2013). Interpyramid spike transmission stabilizes the sparseness of recurrent network activity. *Cereb Cortex* **23**, 293–304.
- Jadhav SP, Kemere C, German PW & Frank LM (2012). Awake hippocampal sharp-wave ripples support spatial memory. *Science* **336**, 1454–1458.
- Ji D & Wilson MA (2007). Coordinated memory replay in the visual cortex and hippocampus during sleep. *Nat Neurosci* **10**, 100–107.
- Klausberger T, Magill PJ, Márton LF, Roberts JD, Cobden PM, Buzsáki G & Somogyi P (2003). Brain-state- and cell-type-specific firing of hippocampal interneurons in vivo. *Nature* **421**, 844–848.
- Kubota D, Colgin LL, Casale M, Brucher FA & Lynch G (2003). Endogenous waves in hippocampal slices. *J Neurophysiol* **89**, 81–89.
- Kwan AC & Dan Y (2012). Dissection of cortical microcircuits by single-neuron stimulation in vivo. *Curr Biol* **22**, 1459–1467.
- Li CY, Poo MM & Dan Y (2009). Burst spiking of a single cortical neuron modifies global brain state. *Science* **324**, 643–646.
- Lee AK & Wilson MA (2002). Memory of sequential experience in the hippocampus during slow wave sleep. *Neuron* **36**, 1183–1194.
- Maier N, Nimmrich V & Draguhn A (2003). Cellular and network mechanisms underlying spontaneous sharp wave-ripple complexes in mouse hippocampal slice. *J Physiol* **550**, 873–887.
- Maier N, Tejero-Cantero A, Dorn AL, Winterer J, Beed PS, Morris G, Kempter R, Poulet JF, Leibold C & Schmitz D (2011). Coherent phasic excitation during hippocampal ripples. *Neuron* **72**, 137–152.
- Memmesheimer RM (2010) Quantitative prediction of intermittent high-frequency oscillations in neural networks with supralinear dendritic interactions. *PNAS (USA)* **107**, 11092–11097.
- Miles R & Wong RKS (1983). Single neurones can initiate synchronized population discharges in the hippocampus. *Nature* **306**, 371–373.
- Miles R & Wong RKS (1987). Inhibitory control of local excitatory circuits in the guinea-pig hippocampus. *J Physiol* **388**, 611–629.
- Miles R (1990). Synaptic excitation of inhibitory cells by single CA3 hippocampal pyramidal cells of the guinea-pig in vitro. *J Physiol* **428**, 61–77.
- Nicholson C & Freeman JA (1975). Theory of current source-density analysis and determination of conductivity tensor for anuran cerebellum. *J Neurophysiol* **38**, 356–368.
- O'Keefe J & Nadel L (1978). *The Hippocampus as a Cognitive Map*, pp. 150–153. Oxford University Press, Oxford.
- Patel J, Schomberg EW, Berényi A, Fujisawa S & Buzsáki G (2013). Local generation and propagation of ripples along the septotemporal axis of the hippocampus. *J Neurosci* **33**, 17029–17041.
- Prida LM, Huberfeld G, Cohen I & Miles R (2006). Threshold behaviour in the initiation of hippocampal population bursts. *Neuron* **49**, 131–142.
- Sasaki T, Matsuki N & Ikegaya Y (2014). Interneuron firing precedes sequential activation of neuronal ensembles in hippocampal slices. *Eur J Neurosci* **39**, 2771–2783.
- Schlingloff D, Káli S, Freund TF, Hájos N & Gulyás AI (2014). Mechanisms of sharp wave initiation and ripple generation. *J Neurosci* **34**, 11385–98.
- Shadlen MN & Newsome WT (1998). The variable discharge of cortical neurons: implications for connectivity, computation, and information coding. *J Neurosci* **18**, 3870–3896.
- Stark E, Roux L, Eichler R, Senzai Y, Royer S & Buzsáki G (2014). Pyramidal cell-interneuron interactions underlie hippocampal ripple oscillations. *Neuron* **83**, 467–480.
- Svoboda KR, Adams CE & Lupica CR (1999). Opioid receptor subtype expression defines morphologically distinct classes of hippocampal interneurons. *J Neurosci* **19**, 85–95.

Additional information

Competing interests

The authors declare that they have no competing interests.

Author contributions

MB carried out the experiments. MB, MT and RM analysed data. RM advised on the experiments and the analysis. MB, MT and RM wrote the manuscript. All authors have approved the final version of the manuscript and agree to be accountable for all aspects of the work. All persons designated as authors qualify for authorship, and all those who qualify for authorship are listed.

Acknowledgements

We wish to thank A. Bacci, M. Capogna, D. Dupret, A. Gulyás, J. C. Ponce and L. M. Prida for their comments on versions of the manuscript, as well as B. Telenczuk for help with analysis.

Funding

We gratefully acknowledge financial support from INSERM, UPMC, ANR (08MNP006), NIH (MH054671) and ERC (322721), as well as a graduate studentship from ENP and DIM-Ile de France to MT.